

## Article

# Compression Density as an Alternative to Identify an Optimal Moisture Content for High Shear Wet Granulation as an Initial Step for Spheronisation

Selina Ramm<sup>1</sup>, Ruwen Fulek<sup>1</sup>, Veronika Anna Eberle<sup>2</sup>, Christian Kiera<sup>2</sup>, Ulrich Odefey<sup>1</sup>  
and Miriam Pein-Hackelbusch<sup>1,\*</sup>

<sup>1</sup> Department of Life Science Technologies, OWL University of Applied Sciences and Arts, Campusallee 12, 32657 Lemgo, Germany

<sup>2</sup> PHARBIL Pharma GmbH, Reichenbergerstr. 43, 33605 Bielefeld, Germany

\* Correspondence: miriam.pein-hackelbusch@th-owl.de

**Abstract:** Pellet production is a multi-step manufacturing process comprising granulation, extrusion and spheronisation. The first step represents a critical control point, since the quality of the granule mass highly influences subsequent process steps and, consequently, the quality of final pellets. The most important parameter of wet granulation is the liquid requirement, which can often only be quantitatively evaluated after further process steps. To identify an alternative for optimal liquid requirements, experiments were conducted with a formulation based on lactose and microcrystalline cellulose. Granules were analyzed with a Powder Vertical Shear Rig. We identified the compression density ( $\rho_{\text{press}}$ ) as the said alternative, linking information from the powder material and the moisture content ( $R^2 = 0.995$ ). We used  $\rho_{\text{press}}$  to successfully predict liquid requirements for unknown formulation compositions. By means of this prediction, pellets with high quality, regarding shape and size distribution, were produced by carrying out a multi-step manufacturing process. Furthermore, the applicability of  $\rho_{\text{press}}$  as an alternative quality parameter to other placebo formulations and to formulations containing active pharmaceutical ingredients (APIs) was demonstrated.

**Keywords:** wet granulation; liquid requirement; granulation endpoint; compression density



**Citation:** Ramm, S.; Fulek, R.; Eberle, V.A.; Kiera, C.; Odefey, U.; Pein-Hackelbusch, M. Compression Density as an Alternative to Identify an Optimal Moisture Content for High Shear Wet Granulation as an Initial Step for Spheronisation.

*Pharmaceutics* **2022**, *14*, 2303.

<https://doi.org/10.3390/pharmaceutics14112303>

Received: 28 September 2022

Accepted: 21 October 2022

Published: 26 October 2022

**Publisher's Note:** MDPI stays neutral with regard to jurisdictional claims in published maps and institutional affiliations.



**Copyright:** © 2022 by the authors. Licensee MDPI, Basel, Switzerland. This article is an open access article distributed under the terms and conditions of the Creative Commons Attribution (CC BY) license (<https://creativecommons.org/licenses/by/4.0/>).

## 1. Introduction

In the pharmaceutical industry granulation is used as a process for size enlargement of small particles. For the granulation of pharmaceutical solids, wet granulation is often applied. This process starts with mixing dry powder, followed by wetting and nucleation once the liquid is added. The nuclei form the basis for the following granule growth and consolidation. If too much liquid is added, granules become a wet mass or slurry due to oversaturation [1,2]. It can thus be concluded that the moisture content is a key factor for the quality of granules [3]. The amount of liquid determines the degree of saturation in the granule structure. The saturation degree is defined by the percentage of intragranular voids filled with liquid and can be described by three states of granules. With increasing liquid loading, the structure changes from pendular, over funicular to capillary state as the saturation reaches 100% [2]. Beyond full saturation, powder particles become suspended in a continuous liquid phase [4].

A critical unit operation is the determination of liquid requirement as there is no intrinsic endpoint. In fact, the optimal endpoint depends on the desired properties of the granules [5], on process conditions and the applied equipment [1], and on the physical properties of the dry raw materials, such as solubility, surface area, particle shape and size distribution. These properties influence the packing pattern of the powder mixture and, thus, the degree of densification and, consequently, the saturation level of the mixture associated with the liquid requirement [2,6].

Therefore, many different approaches exist for determining the required moisture content for granules. An objective method is estimating the required liquid amount by applying a mathematical calculation. For this purpose, Leuenberger et al. [7] developed the following equation.

$$\omega_{dry} = \frac{\rho_l \cdot \varepsilon \cdot \bar{\gamma}}{\rho_s \cdot (1 - \varepsilon)} + \delta \quad (1)$$

In Equation (1),  $\omega_{dry}$  is the required water content on a dry basis,  $\varepsilon$  is the porosity of the tapped powder,  $\rho_l$  is the density of the liquid,  $\rho_s$  is the true density of the solid.  $\bar{\gamma}$  corresponds to a mean complete formation of liquid bridges in the pile and  $\delta$  is the equilibrium moisture content of the product at 100% air humidity. Limitations for the use of this equation are, on the one hand, porosity  $\varepsilon$  to be estimated on the basis of the tapped density. On the other hand, for  $\bar{\gamma}$ , the packing of the particles to be either cubic or rhombohedral has to be estimated, as well as the degree of filling pore spaces. Furthermore, this calculation only provides the optimal moisture content related to the saturation level, but it does not consider the mechanical properties of the granules.

These properties are even more important if granules are further processed [8], for example, during tableting or extrusion. In a multi-step manufacturing process, such as pellet production, granulation is followed by extrusion and spheronization. The liquid requirement of the initial granule mass thus directly correlates with the pellet quality [3]. The so-called hand pressure test is, for this reason, typically applied during formulation development. In this test, the granules are compressed by hand, and if the mass does not crumble, the amount of liquid is suitable for further processing [9–12]. The main disadvantage of this method is the subjectivity and the required experience needed to reproducibly perform this test. A scientifically sound upgrade of this method is the torque rheological characterization performed with a mixing torque rheometer [11,13–15]. The changes in torque thereby display the resistance of the granule mass relative to mixing. Plotting changes in torque against the binder ratio allows identifying different wetting phases during granulation. Moreover, the binder ratio yielding the maximum change in torque was identified as optimal [13–15]. This optimal value has also been shown to be relevant for extrusion–spheronization [11]. Indirectly, the liquid requirement can also be evaluated by physical properties of the granules, such as bulk and tapped density and the resulting Carr's compressibility index [16–18]. The disadvantage is that the samples must first be dried before standard analytical methods; for example, sieving for particle sizing can be used.

In our work, we aimed to identify an alternative parameter that can predict the quality of the pellets already during granulation by means of the liquid requirement of the formulation. Based on a placebo formulation, a suitable alternative quality parameter, connected with the formulation's composition and with the moisture content, should be identified. The applicability of this parameter should be verified by predicting liquid requirements for further formulation compositions. In addition, we wanted to carry out extrusion and spheronization based on predicted moisture contents and to discuss the quality of resulting pellets. Since formulations containing active pharmaceutical ingredients (APIs) are more commonly produced in the industry than placebo formulations, initial experiments should be conducted to assess whether the identified parameter could also be applied for API formulations.

## 2. Materials and Methods

The applied raw materials used in this study (lactose grades, mannitols, microcrystalline celluloses and APIs) are summarized in Table 1.

**Table 1.** Raw materials used in this study.

Material	Type	Abbreviation	Company
Lactose anhydrate	DuraLac <sup>®</sup> H	Lac H	Meggle, Wasserburg, Germany
	Pharmatose <sup>®</sup> DCL 21	Lac DCL 21	DMV International, Veghel, The Netherlands
A Lactose monohydrate	GranuLac <sup>®</sup> 70	Lac 70	Meggle, Wasserburg, Germany
	GranuLac <sup>®</sup> 200	Lac 200	Meggle, Wasserburg, Germany
	Pharmatose <sup>®</sup> 200M	Lac 200M	DFE Pharma, Goch, Germany
	SorboLac <sup>®</sup> 400	Lac 400	Meggle, Wasserburg, Germany
Mannitol	D(-)-Mannit	Man	Merck, Darmstadt, Germany
	PEARLITOL <sup>®</sup> 50 C	Man 50 C	Roquette Frères, Lestrem, France
B Microcrystalline cellulose	Microcel <sup>®</sup> MC-101	MCC MC-101	Roquette Frères, Lestrem, France
	VIVAPUR <sup>®</sup> 101	MCC 101	JRS Pharma, Rosenberg, Germany
	VIVAPUR <sup>®</sup> 102	MCC 102	JRS Pharma, Rosenberg, Germany
	VIVAPUR <sup>®</sup> 105	MCC 105	JRS Pharma, Rosenberg, Germany
API Active pharm. ingredient	Caffeine (pure) (2.0 $\mu\text{m} \pm 0.4 \mu\text{m}$ ; $n = 17$ ) *		Merck, Darmstadt, Germany
	Ibuprofen 25 (52.4 $\mu\text{m} \pm 25.9 \mu\text{m}$ ; $n = 17$ )		BASF, Ludwigshafen, Germany
	Ketoprofen (2.8 $\mu\text{m} \pm 0.6 \mu\text{m}$ ; $n = 17$ )		Hubei Xunda Pharmaceutical, Wuxue, China
	Paracetamol (19.5 $\mu\text{m} \pm 15.6 \mu\text{m}$ ; $n = 48$ )		Merck, Darmstadt, Germany

\* Mean particle size with standard deviation and sample size ( $n$ ). Particle size was measured by suspending the sample in paraffin and measuring it using a microscope (Olympus BX41).

### 2.1. Granulation Equipment

Granulation was performed in a Thermomix<sup>®</sup> TM6 (Vorwerk, Wuppertal, Germany) with a bowl size of 2.2 L. According to the manufacturer, the impeller's speed can be adjusted from 40 rpm to 10,700 rpm [19]. In our study, we adjusted the impeller speed at 150 rpm. We replaced the original agitator by a custom-made mixing knife. The original Thermomix mixing knife was adapted by cutting off four mixing knives; then, stirring blades with dimensions of 4.5 cm  $\times$  1.5 cm  $\times$  0.2 cm were welded at an angle of 45°. This modification ensured proper material mixing and mimicked Diosna's P 1–6 intensive mixer (DIOSNA Dierks & Söhne, Osnabrück, Germany). Water was added via a peristaltic pump (1B.1003-R/65, Petro Gas, Berlin, Germany). The inner diameter of the tube was 5 mm and equipped with a nozzle with an inner diameter of 1 mm. The amount of water added was controlled with a scale (PCE-BS 3000, PCE Instruments<sup>™</sup>, Meschede, Germany).

### 2.2. Granulation in Lab-Scale

A dry mass of 150 g was used for each batch. Dry materials were passed through a 1400  $\mu\text{m}$  sieve and transferred to the mixing bowl. After dry mixing for 3 min in the Thermomix<sup>®</sup> TM6 (see Section 2.1) with an impeller speed of 150 rpm, water was added with 15 mL  $\text{min}^{-1}$ , while keeping the impeller's speed constant. The time for water addition was dependent on the amount of water. For example, with a dry mass of 150 g and a target water content on wet basis ( $\omega_{\text{wet}}$ ) of 20%, the addition time was 2.5 min (37.5 g water). To ensure the preparation of homogeneous samples after all water was added, the mixing process stopped and material adhering to the mixing bowl was scraped off manually. Subsequently, larger agglomerates were crushed at a speed of 2000 rpm for 3 s. For each formulation, one batch was performed and samples were taken for the respective  $\omega_{\text{wet}}$ . The sample size was 38 g so that the compression density ( $\rho_{\text{press}}$ ) could be determined in

triplicates (12 g each). The experimental procedure is summarized in Table 2. For details on the raw materials (abbreviated with A, B and API), we refer to Table 1.

**Table 2.** Experimental procedure. Abbreviations and labeling can be found in Table 1.

Combination of Raw Materials	Raw Material Ratio	$\omega_{\text{wet}}$ *
Lac 200:MC 101 <sup>1</sup>	0:100–100:0	see Table A1
Lac 200:MC 101 <sup>2</sup>	80:20	0–45%
A:MCC 101	80:20 and 60:40	0%, 15%, 22.5%, 30%
Lac 200:B	80:20 and 60:40	0%, 15%, 22.5%, 30%
API:Lac 200:MCC 101	40:40:20	0%, 15%, 22.5%, 30%

\*  $\omega_{\text{wet}}$  is the water content on wet basis. <sup>1</sup> Formulation with 100% Lac 200: use of 180 g dry mass instead of 150 g.

<sup>2</sup> Three batches; each batch n = 1.

### 2.3. Measurement of $\rho_{\text{press}}$

A Texture Analyser (TA.XTplus, Stable Mirco Systems, Godalming, UK) with a 50 kg load cell and a Powder Vertical Shear Rig (A/PVS) was used to determine  $\rho_{\text{press}}$ . For each analysis, 12 g of granulate was weighed in and transferred to the body of the rig and compressed with 196 N for 20 s. The final height of the compressed material was registered. For data recording and evaluation, software Exponent (Stable Mirco Systems, Godalming, UK) was used.

### 2.4. Proof of Concept: Pellet Production in Lab-Scale

For the multi-step manufacturing process of granulation, extrusion, spheronization and drying, a total dry mass of 500 g per batch was used. Granulation was carried out in the Bosch MUM6712 (Robert Bosch Hausgeräte GmbH, München, Germany) with a bowl size of 5.3 L, equipped with twin beating whisks. Bosch MUM6712 was qualified for accurate impeller speed (with a maximum deviation of  $\pm 3\%$ ) over the entire working range. After 5 minutes of dry mixing at agitator level 1 (impeller speed without load is 95 rpm; under load, the speed decreases), water was added by hand (for example, about 3 min for 200 g water), followed by another 5 minutes of mixing. Extrusion was performed using Schlüter Extruder PP85 (Maschinenfabrik H. Schlüter GmbH, Neustadt a. Rbge., Germany) with a MA9/085-003 die and 0.1 mm collar distance at 500 rpm. The screen size was 85 mm in diameter, and each bore had a diameter of 1.0 mm and a bore length of 2.0 mm. Schlüter RM300 (Maschinenfabrik H. Schlüter GmbH, Neustadt a. Rbge., Germany) was used as the spheronizer. Spheronization was performed at 434 rpm for 1 min, 665 rpm for 1 min, 786 rpm for 3 min and at 1028 rpm for 5 min. The diameter of the spheronizer disc was 300 mm. Drying was carried out overnight at 50 °C in the drying cabinet HORO 200 (HORO Dr. Hofmann GmbH, Ostfildern, Germany). The residual moisture content was determined with the Mettler Toledo Moisture Analyser HG83 (Mettler Toledo AG, Greifensee, Schweiz). In detail, sample sizes of 3 g pellets were measured at 105 °C. The measurement stopped as soon as the mean weight loss over 50 s was less than 1 mg. Determined residual moisture contents of the pellets are summarized in Table A2. Sieving for particle size distribution was performed by the manual removal of over- and under-sized pellets using 0.8/1.6 mm (1.6/4.0 mm) Kressner sieves. Sieve analysis of in sized fraction (0.8–1.6 mm) was performed with the JEL exzenter lab sieving machine (J. Engelsmann, Ludwigshafen, Germany). The sieve stack of 0.8/1.0/1.25/1.4/1.6 mm was loaded with 25 g for 5 min. For presentation, the results were combined into two fractions (0.8–1.6 mm and 1.6–4.0 mm).

### 2.5. Statistical Analysis

$\rho_{\text{press}}$  measurements were performed in triplicates. Statistical analyses were performed by one-way ANOVA. A *p*-value smaller than 0.05 was considered statistically significant.

Statistical analyses were performed using Minitab<sup>®</sup> 20.4. All experimental data are presented as mean  $\pm$  standard deviation ( $n = 3$ ).

### 3. Results and Discussion

#### 3.1. Identification of a Moisture Related Quality Parameter for Granules

The quality of the granule mass prior pelletisation is often determined by the hand pressure test and, thus, by the behavior of the granules under/after compression. We therefore utilized the at-line capable measuring method of the Texture Analyser with the Powder Vertical Shear Rig, which allowed the measurement of various parameters of the granulated material under compression and under shear. During the test, the powder is compressed under defined conditions (Section 2.3), yielding  $\rho_{\text{press}}$ . In a subsequent step of the test, a trap door underneath the powder cake opened. A piston then pushes (powder shear speed  $0.5 \text{ mm s}^{-1}$ , distance 5 mm) a plug of the powder cake through this opening. During the entire process, the drag force is recorded (Figure 1, left part). Here, the area under the curve, the maximum force and the vertical shear strength are monitored. The area under the curve is provided by the integral of the curve section resulting from the shearing process (Figure 1, area highlighted in gray) and the maximum force corresponds to the local maximum of this curve section (Figure 1 right part). The vertical shear strength is the ratio of the max. force and the lateral surface area of the briquette (Equation (2)). Detailed information about the described measurement has been published in [20].

$$\text{vertical shear strength} = \frac{\text{max. force}}{\text{lateral surface area}} \quad (2)$$

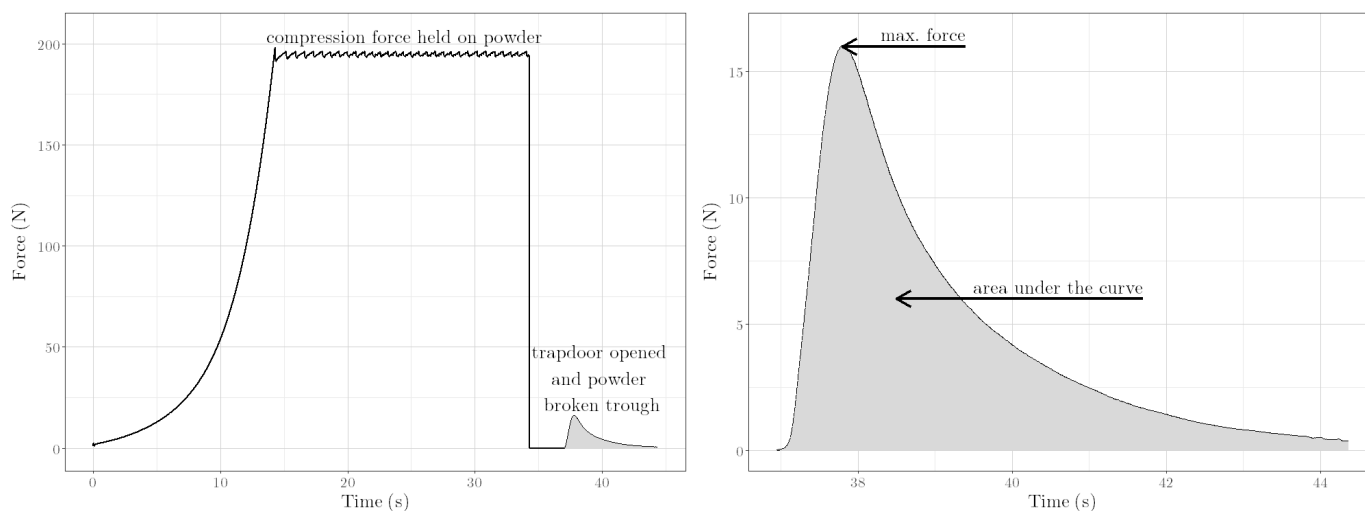


**Figure 1.** Measurement curve of the Powder Vertical Shear Test (formulation with 80:20 Lac 200:MCC 101 ratio and  $\omega_{\text{wet}}$  15%), performed with the Texture Analyser TA.XTplus with the Powder Vertical Shear Rig. **(Left):** Entire curve. **(Right):** Curve section, resulting from the shearing process. Highlighted in gray: Area under the curve.

Since we sought an alternative parameter for the quality of the granules related to their extrudability and spheronizability, it was expected that the parameters resulting from the shear of the granules would be suitable. However, experiments based on different formulations (Table A1) demonstrated that the area under the curve, max. force and shear strength are not suitable (Figure 2). Only  $\rho_{\text{press}}$  showed a clear dependence on both the formulation and moisture content.

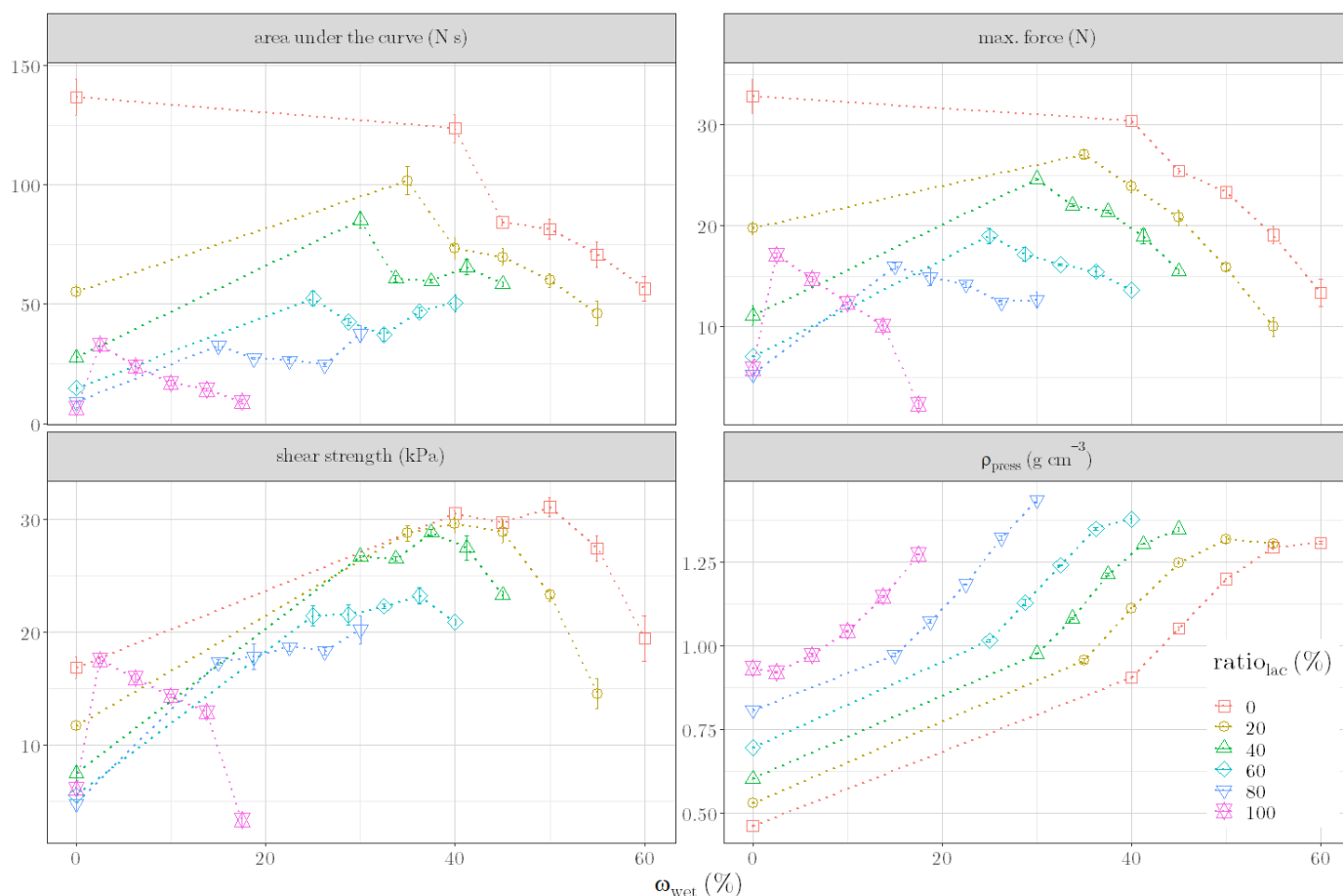


**Figure 2.** Area under the curve, max. force, shear strength and compression density ( $\rho_{\text{press}}$ ) versus  $\omega_{\text{wet}}$  for formulations with 0%, 20%, 40%, 60%, 80% and 100% lactose ratio in the dry formulation ( $\text{ratio}_{\text{lac}}$ ).

In detail, the lactose ratio in the dry formulation ( $\text{ratio}_{\text{lac}}$ ) positively correlates with  $\rho_{\text{press}}$ . This observation is in good agreement to the tapped density of two raw materials. For Lac 200, the tapped density is  $0.82 \text{ g cm}^{-3}$  [21] and the measured  $\rho_{\text{press}}$  is  $0.93 \text{ g cm}^{-3}$  ( $\text{ratio}_{\text{lac}}$  100%). For MCC 101, the tapped density is  $0.42 \text{ g cm}^{-3}$  [22] and the measured  $\rho_{\text{press}}$  is  $0.46 \text{ g cm}^{-3}$  ( $\text{ratio}_{\text{lac}}$  0%). It could be assumed that the higher the tapped density of the raw material, the higher  $\rho_{\text{press}}$  is. However, the tapped density is not exactly the same as  $\rho_{\text{press}}$ . In both density measurements, particles are rearranged by externally applied forces (tapping or pressing). In the case of  $\rho_{\text{press}}$ , the pressure can also lead to structural changes in particles due to breakage. Fractures due to applied pressure occur in brittle materials, such as lactose and mannitol. MCC, on the other hand, exhibits plastic deformation behavior and is not subject to fracture effects [23,24]. Thus, the differences between the tapped density and the measured  $\rho_{\text{press}}$  of 11% for Lac 200 and 9% for MCC 101 exhibit the higher compressibility of Lac 200 to MCC 101, which is caused by breakage during compression whereby small fragments fill the inter-particulate pore's space.

In detail, the dependence of  $\rho_{\text{press}}$  on  $\omega_{\text{wet}}$  is shown in Figure 3. At a constant  $\text{ratio}_{\text{lac}}$ ,  $\rho_{\text{press}}$  increases with increasing  $\omega_{\text{wet}}$ , whereby a sigmoidal dependence can be recognized. After compressing the dry powder mixture, air-filled cavities are still present. These are filled with liquid when compressing moist granules, resulting in a higher  $\rho_{\text{press}}$ . If all cavities are completely filled with liquid,  $\rho_{\text{press}}$  cannot increase further but remains constant. Related to the states of the granules described in the introduction, the graph in Figure 3 represents the pendular state in the first exponential section up to 15%  $\omega_{\text{wet}}$ . Here, intra-particulate pore spaces are initially filled with water, which only leads to minor

changes in  $\rho_{\text{press}}$ . At the transition from filling the intra-particulate pore spaces to filling inter-particulate pore spaces with liquid, the graph changes from the exponential section to the linear section. This section from 15% to 30%  $\omega_{\text{wet}}$  represents the funicular state. The capillary state, where liquid saturation occurs, is described by the last section of the graph from 30% to 45%  $\omega_{\text{wet}}$ . This sigmoidal progression of  $\rho_{\text{press}}$  over  $\omega_{\text{wet}}$  is similar to the change in power consumption with increasing moisture contents during granulation, as described by Leuenberger [7].

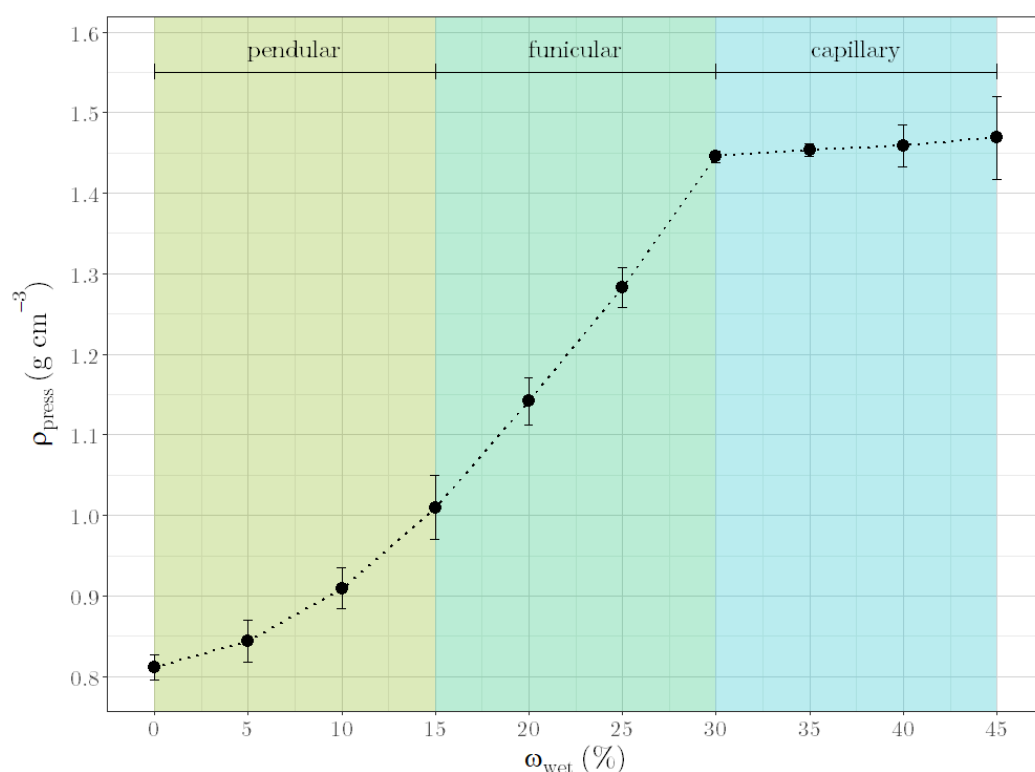


**Figure 3.**  $\rho_{\text{press}}$  versus  $\omega_{\text{wet}}$  for a formulation with Lac 200 and MCC 101 in a ratio of 80:20. Granulation states are color annotated.

### 3.2. Prediction for a Standard Placebo Formulation with Different Ratios of Lac 200 and MCC 101 and Various Moisture Contents

Once  $\rho_{\text{press}}$  was found to show a correspondence with formulation compositions as well as with moisture content, the suitability of this alternative quality parameter should be verified by predicting the liquid requirement for further formulation compositions.

Based on the data from Figure 2, we used a multivariate regression model (Equation (3)) to estimate a relationship between  $\text{ratio}_{\text{lac}}$ ,  $\omega_{\text{wet}}$  and  $\rho_{\text{press}}$  ( $p < 0.05$ ).

$$\begin{aligned} \rho_{\text{press}} = & 0.465 + 0.002785 \text{ ratio}_{\text{lac}} - 0.06206 \omega_{\text{wet}} \\ & + 0.0007451 \text{ ratio}_{\text{lac}} \cdot \omega_{\text{wet}} + 0.00001762 \text{ ratio}_{\text{lac}}^2 \\ & + 0.00294 \omega_{\text{wet}}^2 - 0.000001148 \text{ ratio}_{\text{lac}}^2 \cdot \omega_{\text{wet}} \\ & - 0.00001393 \text{ ratio}_{\text{lac}} \cdot \omega_{\text{wet}}^2 - 0.00002793 \omega_{\text{wet}}^3 \end{aligned} \quad (3)$$

This model provided a coefficient of determination,  $R^2$ , of 0.995 and a standard deviation of about  $0.0178 \text{ g cm}^{-3}$ . The model is accurate, especially in the range of  $0.95 \text{ g cm}^{-3} < \rho_{\text{press}} < 1.35 \text{ g cm}^{-3}$ , corresponding to realistic values.

For a typical placebo formulation in industry (80:20 Lac:MCC ratio, 25%  $\omega_{\text{wet}}$ ), which shows good extrudability and spheronizability, a  $\rho_{\text{press}}$  of  $1.26 \text{ g cm}^{-3}$  was determined.

Using Equation (3), we predicted the required  $\omega_{\text{wet}}$  for three different so-far untested formulations to obtain a  $\rho_{\text{press}}$  of  $1.26 \text{ g cm}^{-3}$ . Solving Equation (3) for  $\omega_{\text{wet}}$  yields three solutions, two of which are discarded because their values are outside the valid range of  $\omega_{\text{wet}}$ . For Lac:MCC ratios of 30:70, 55:45 and 72:28, the valid solutions for  $\omega_{\text{wet}}$  are 43.2%, 34.3% and 28.0%, respectively. The results of the experiments under predicted conditions are shown in Table 3.

The  $\rho_{\text{press}}$  of the three formulations resulting from the predicted water contents lie within the confidence interval of the prediction (Table 3). This indicates that the regression model is valid and that  $\rho_{\text{press}}$  is suitable for predicting liquid requirements for binary formulations of Lac 200 and MCC 101.

**Table 3.** Obtained  $\rho_{\text{press}}$  as means with corresponding standard deviations (SD) and confidence intervals of the experiments under predicted conditions.

Lac:MCC Ratio	$\rho_{\text{press}}$ ( $\text{g cm}^{-3}$ )		
	Mean ( $n = 3$ )	SD	95%-Confidence Interval
30:70	1.262	$\pm 0.00393$	[1.252; 1.268]
55:45	1.264	$\pm 0.00318$	[1.254; 1.266]
72:28	1.253	$\pm 0.00130$	[1.253; 1.267]

### 3.3. Proof of Concept for Standard Placebo Formulations

To show the applicability of  $\rho_{\text{press}}$  as an alternative measure of spheronizability, the processability of different formulations was assessed. For this purpose, the  $\omega_{\text{wet}}$ , required to obtain a  $\rho_{\text{press}}$  of  $1.26 \text{ g cm}^{-3}$ , was predicted (Equation (3)) for three further formulations. We also predicted the required  $\omega_{\text{wet}}$  for an over-wetted formulation at the upper limit of the valid range of Equation (3). Formulations and predicted  $\omega_{\text{wet}}$  for the desired  $\rho_{\text{press}}$  are shown in Table 4.

**Table 4.** Predicted  $\omega_{\text{wet}}$  to obtain desired  $\rho_{\text{press}}$  for different formulations.

Formulation	Lac:MCC Ratio	Desired $\rho_{\text{press}}$ ( $\text{g cm}^{-3}$ )	Predicted $\omega_{\text{wet}}$ (%)
(a)	80:20	1.26	25.0
(b)	70:30	1.26	28.7
(c)	60:40	1.26	32.4
(d)	60:40	1.34	35.9

The resulting pellets of the multi-step manufacturing process under predicted conditions are shown in Figure 4. For the formulations with the desired  $\rho_{\text{press}}$  of  $1.26 \text{ g cm}^{-3}$ , the pellets are spherical and show a comparable average particle size (Figure 5). The slightly smaller size of the pellets with a higher MCC content is due to the behavior of the MCC, which tends to intrinsically round out [25]. In contrast, the pellets of the over-wetted formulation are spherical but show a much larger average particle size. This is due to coalescence, as over-wetted materials tend to uncontrolled agglomeration during spheronization, resulting in large pellets [3]. These results underscore that  $\rho_{\text{press}}$  is suitable for assessing the quality of pellets.

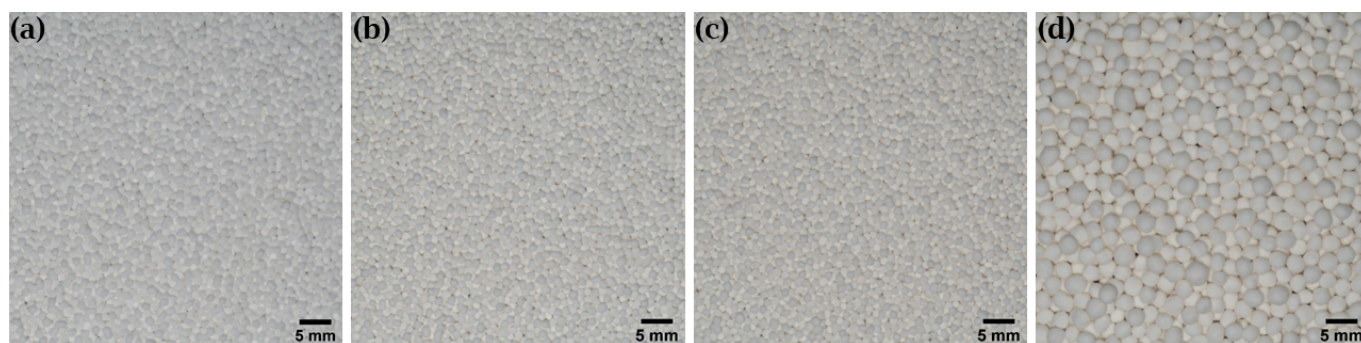


**Figure 4.** Pellets of the multi-step manufacturing process under predicted conditions. (a) Lac:MCC ratio 80:20,  $\omega_{\text{wet}}$  25.0%. (b) Lac:MCC ratio 70:30,  $\omega_{\text{wet}}$  28.7%. (c) Lac:MCC ratio 60:40,  $\omega_{\text{wet}}$  32.4%. (d) Lac:MCC ratio 60:40,  $\omega_{\text{wet}}$  35.9%.

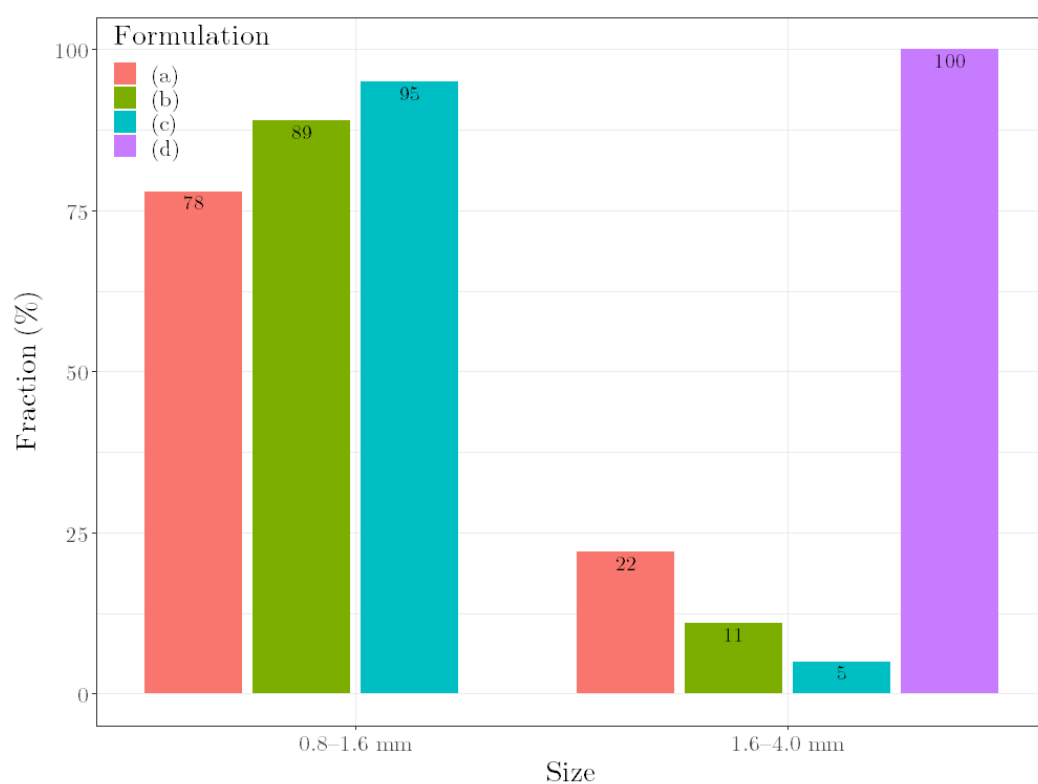


**Figure 5.** Particle size of the pellets of the different formulations. (a) Lac:MCC ratio 80:20,  $\omega_{\text{wet}}$  25.0%. (b) Lac:MCC ratio 70:30,  $\omega_{\text{wet}}$  28.7%. (c) Lac:MCC ratio 60:40,  $\omega_{\text{wet}}$  32.4%. (d) Lac:MCC ratio 60:40,  $\omega_{\text{wet}}$  35.9%.

### 3.4. Applicability of $\rho_{\text{press}}$ for Other Materials

Changing raw material batches or brands during manufacturing can be critical, as small differences in the materials can already have a major impact on the quality of products. After demonstrating that  $\rho_{\text{press}}$  is a suitable quality parameter for formulations as a function of  $\text{ratio}_{\text{lac}}$  and  $\omega_{\text{wet}}$ , the applicability of the parameter to other placebo formulations should be investigated. It is noticeable that lactose monohydrate, lactose anhydrous and mannitol (raw materials A, Table 1) behave comparably with respect to the determined  $\rho_{\text{press}}$  at the same proportion in the formulation and the same  $\omega_{\text{wet}}$  (Figure 6). This is in good agreement with the findings of Roberts and Rowe [26]. They stated that pure and water-free lactose, mannitol and also sucrose are materials with a medium yield pressure that are strain-rate dependent. This behaviour is indicative for moderately hard materials that plastically deform under loading. Only the  $\rho_{\text{press}}$  of formulations with 60% material A

at 30%  $\omega_{\text{wet}}$  show a differentiation between the material types. In detail, the anhydrous lactoses Lac H and Lac DCL 21 show the largest  $\rho_{\text{press}}$ , and mannitol grades and lactose monohydrate grades have comparable  $\rho_{\text{press}}$ . The similar compactibility behavior of formulations based on mannitol and lactose monohydrate is also visualized by the resulting surface of briquettes (Figure 7). However, as there is no significant difference between the  $\rho_{\text{press}}$  of dry formulations with Lac 400 and Lac 70 (both for 60% and for 80%  $\text{ratio}_{\text{lac}}$ ), the former assumption that  $\rho_{\text{press}}$  increases with an increasing tapped density of the raw materials must be put into perspective.

Comparing different materials B (Figure 8), it is noticeable that the  $\rho_{\text{press}}$  of dry formulations differ insofar as the  $\rho_{\text{press}}$  for formulations with MCC 105 are distinctly lower than that of other formulations. This is caused by the very small particle size (the average particle size is 15  $\mu\text{m}$  [27]) and the associated electrostatic effects, which decrease with water addition. However, this influence is minimized when water is added and the  $\rho_{\text{press}}$  converge to the same value with increasing water content. For  $\omega_{\text{wet}} > 15\%$ , the three VIVAPUR<sup>®</sup> products (MCC 101, MCC 102, and MCC 105) behave comparably with respect to the determined  $\rho_{\text{press}}$  at the same proportion in the formulation. At contents of 20% and 40% and a  $\omega_{\text{wet}} \geq 22.5\%$ , MCC MC-101 has a lower  $\rho_{\text{press}}$  than the other celluloses tested. This difference could result from the different manufacturer. MCC MC-101 is spray-dried [28], whereas the other celluloses are air-stream-manufactured [22]. These observations agree with Kleinebudde [3], who summarized that the particle size of MCC has only a minor effect on the liquid requirement, whereas different manufacturers and material sources have a much greater influence. In addition, other studies already described that celluloses of the same grade exhibit differences in their physicochemical properties [22,29].

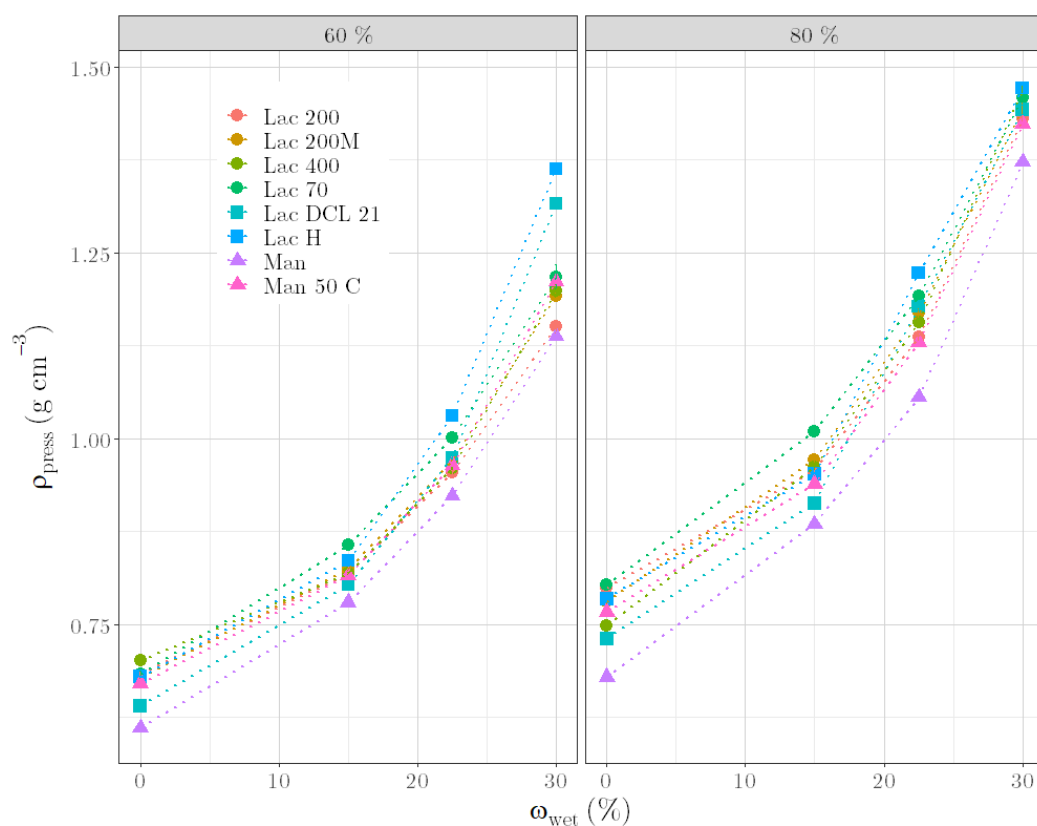


**Figure 6.**  $\rho_{\text{press}}$  versus  $\omega_{\text{wet}}$  for formulations with different raw material A according to 60% (left) and 80% (right) content.

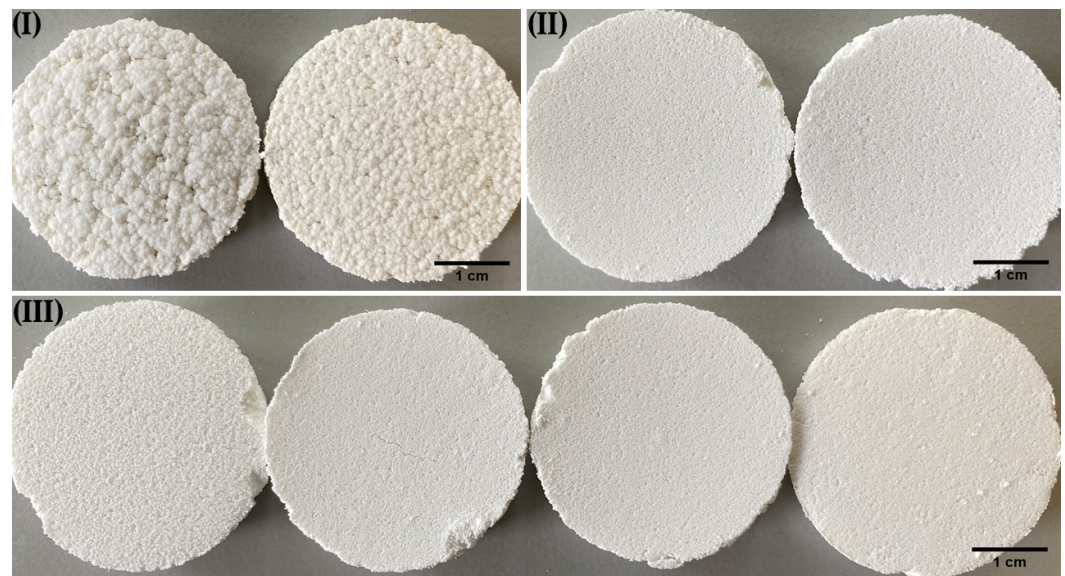


**Figure 7.** Surfaces of the briquettes with 60% ratio<sub>lac</sub> and 30%  $\omega_{wet}$ . Left to right: (I) Lac H and Lac DCL 21. (II) Man and Man 50 C. (III) Lac 70, Lac 200, Lac 200M and Lac 400.

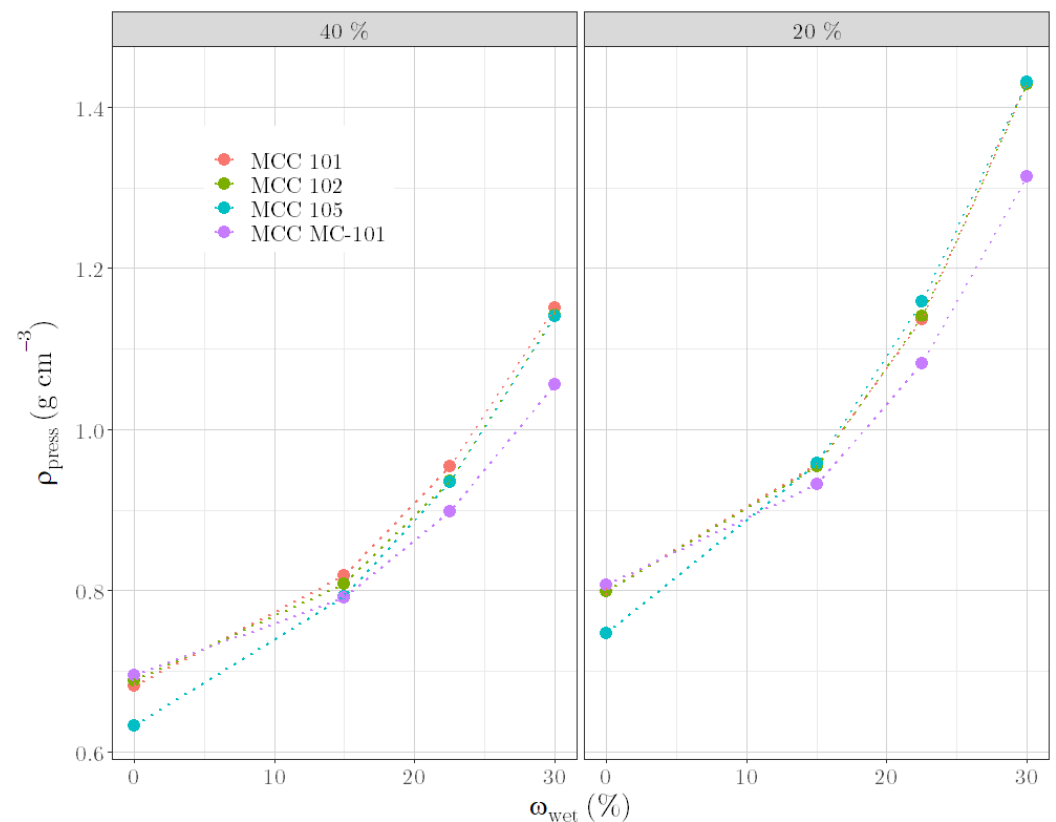


**Figure 8.**  $\rho_{press}$  versus  $\omega_{wet}$  for formulations with different raw materials B according to 40% (left) and 20% (right) content.

### 3.5. Perspective for API Containing Formulations

Pharmaceutical manufacturer typically produce API-containing formulations rather than placebo formulations. We thus performed first experiments to assess whether  $\rho_{press}$  could also be applied for API formulations. Again, we found that  $\rho_{press}$  increases with increasing  $\omega_{wet}$ , independent of the evaluated API formulations (Figure 9). For the purpose of alignment, the area highlighted in gray shows the range between the measured values

of the placebo formulation with Lac 200 and MCC 101 in a ratio of 60:40 (lower limit) and 80:20 (upper limit). The data of the ternary formulations lie in the highlighted area or slightly below. This shows that even with the use of APIs, the values of  $\rho_{\text{press}}$  have a comparable order of magnitude. For a more accurate assessment, the API content in the formulation has to be increased in further trials and additional APIs have to be tested. This first insight nevertheless indicates the possibility of transferring the diagnostic ability of the  $\rho_{\text{press}}$  measurement to ternary formulations with APIs.

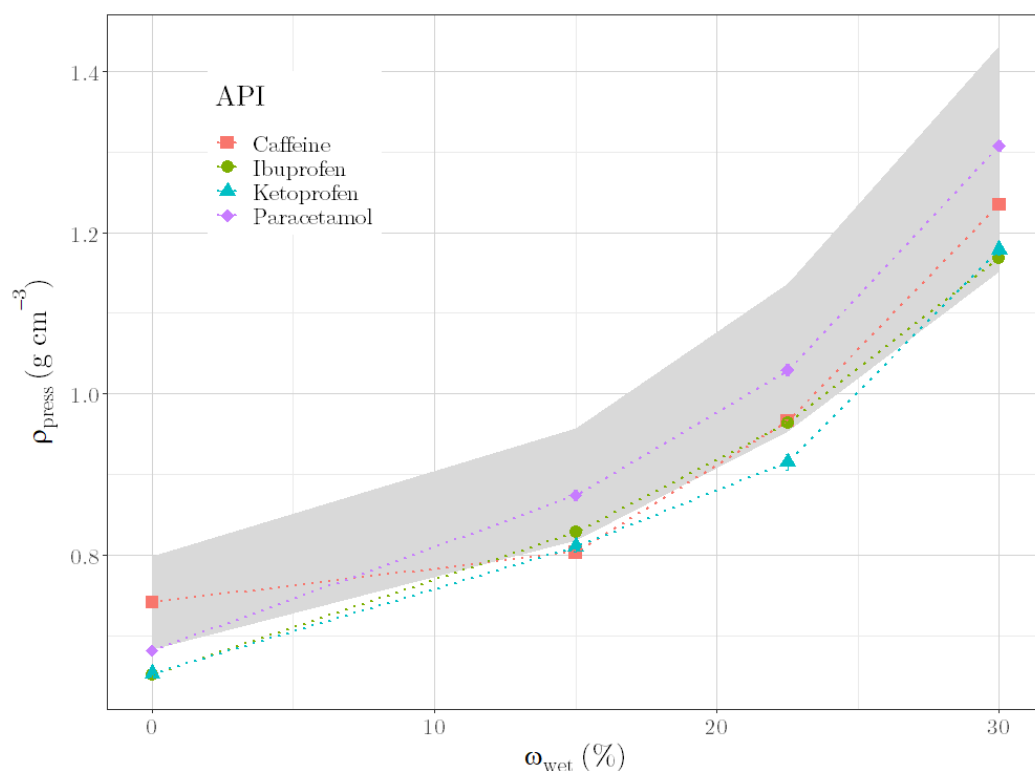


**Figure 9.**  $\rho_{\text{press}}$  versus  $\omega_{\text{wet}}$  for ternary formulations with 40% API, 40% Lac 200 and 20% MCC 101. Highlighted in gray: range between the measured values of the binary formulation with Lac 200 and MCC 101 in a ratio of 60:40 (lower limit) and 80:20 (upper limit).

### 3.6. Proof of Concept for Other Materials

As an example, the pellet's production in lab-scale was carried out for formulations with Lac 400 (representative for lactose monohydrate), Lac DCL 21 (representative for lactose anhydrate) and Man 50 C (representative for mannitol) with MCC 101 at a ratio of 60:40. Representative for API, a formulation with Paracetamol at a ratio of 40:40:20 with Lac 200 and MCC 101 was used. We used the datapoints of  $\rho_{\text{press}}$  at 22.5% and 30% water content (Figures 6 and 9) to calculate  $\omega_{\text{wet}}$  required to achieve a  $\rho_{\text{press}}$  of  $1.26 \text{ g cm}^{-3}$ . Formulations and the estimated values for  $\omega_{\text{wet}}$  for the desired  $\rho_{\text{press}}$  are shown in Table 5.

**Table 5.** Estimated  $\omega_{\text{wet}}$  to obtain a  $\rho_{\text{press}}$  of  $1.26 \text{ g cm}^{-3}$  for different formulations.

Formulation	Estimated $\omega_{\text{wet}}$ (%)
(a) 60% Lac 400, 40% MCC 101	31.9
(b) 60% Lac DCL 21, 40% MCC 101	28.8
(c) 60% Man 50 C, 40% MCC 101	31.5
(d) 40% Paracetamol, 40% Lac 200, 20% MCC 101	28.7

The resulting pellets of the multi-step manufacturing process, using the parameter values calculated above, are shown in Figure 10. The formulation with lactose monohydrate shows the smallest pellet size, followed by lactose anhydrous and mannitol. An effect of the particle size of the applied materials (see Table 1 and information in the product data sheets) on the quality of the pellets could not be observed. However, it appears that the increase in the strain rate's sensitivity index [26] directly correlates with the increase in pellet size. The formulation with paracetamol shows the largest pellets. This finding is not in agreement with the strain rate sensitivity index presented by Roberts and Rowe [26], which might be due to the fact that they analyzed spray-dried Paracetamol with 4% hydrolysed gelatin. However, Paracetamol in contrast to lactose, and mannitol is regarded as highly elastic [30]. As it was noticed during extrusion that all four formulations extrude very well and smoothly, straight strands were produced, and a smaller diameter of the extrusion die could have led to an acceptable pellet size for Paracetamol-loaded pellets. Thus, it can be assumed that, for different formulations, a  $\rho_{\text{press}}$  of  $1.26 \text{ g cm}^{-3}$  is a suitable indicator for the extrudability of the granules. In summary, a  $\rho_{\text{press}}$  of  $1.26 \text{ g cm}^{-3}$  can be regarded as a type of anchor for good extrudability, from which the fine adjustment of the moisture content and/or the equipment can be made depending on the desired pellet size.

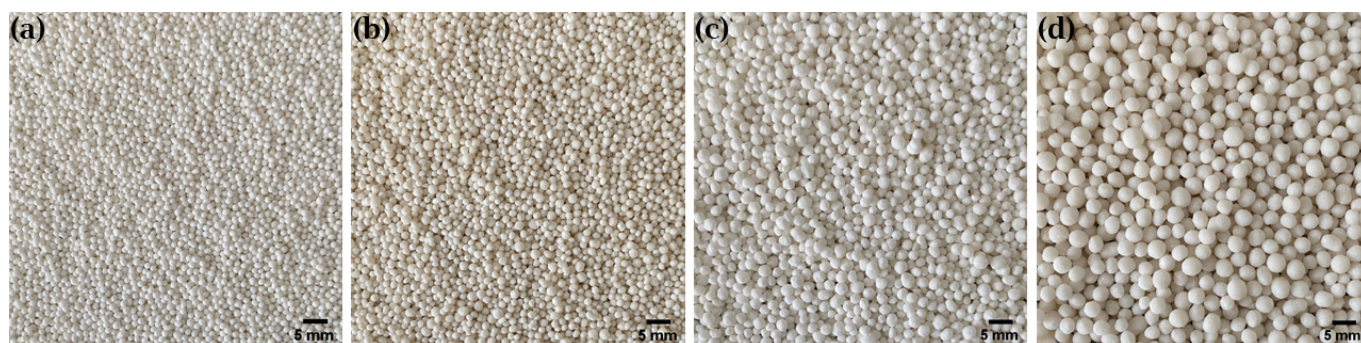


**Figure 10.** Pellets of the multi-step manufacturing process. (a) Lac 400:MCC 101 ratio 60:40,  $\omega_{\text{wet}}$  31.9%. (b) Lac DCL 21:MCC 101 ratio 60:40,  $\omega_{\text{wet}}$  28.8%. (c) Man 50 C:MCC 101 ratio 60:40,  $\omega_{\text{wet}}$  31.5%. (d) Paracetamol:Lac 200:MCC 101 ratio 40:40:20,  $\omega_{\text{wet}}$  28.7%.

#### 4. Conclusions

To evaluate the quality of the granules during granulation, the  $\rho_{\text{press}}$  of the granule mass was identified as an alternative parameter. This parameter showed a relation with formulation compositions as well as with moisture content. A regression model, based on this relation, was successfully used to predict liquid requirements for unknown formulation compositions. In addition, uniform pellets were produced by carrying out the multi-step manufacturing process of granulation, extrusion and spheronization with the predicted liquid requirements for different formulations. Since these results could verify the suitability of  $\rho_{\text{press}}$  as an alternative quality parameter, the applicability of the parameter to other placebo formulations was demonstrated. Moreover, first experiments with API formulations suggested the applicability to industrially relevant formulations. In conclusion, the results indicate that once a  $\rho_{\text{press}}$  is defined for an optimal formulation, changes in material batches and even material types could be compensated with the right amount of water. However, one remaining question is which material properties, in addition to the tapped density and the brittleness, influence  $\rho_{\text{press}}$  or correlate with it. If defined material properties could be determined,  $\rho_{\text{press}}$  would not have to be defined for an optimal formulation but could be determined generally for corresponding material properties. One remaining disadvantage of the presented method is that the optimal  $\rho_{\text{press}}$  for ideal further processing depends on the process parameters of the further processing itself (such as the extruder die). Therefore, no generally valid statement can be made about an optimal  $\rho_{\text{press}}$ ; this must be individually adapted to the multi-step manufacturing process' parameters used.

**Author Contributions:** Conceptualization, S.R. and M.P.-H.; methodology, S.R. and R.F.; formal analysis, S.R.; investigation, S.R., V.A.E. and C.K.; resources, V.A.E. and C.K.; writing—original draft preparation, S.R. and M.P.-H.; writing—review and editing, S.R., R.F., V.A.E., C.K., U.O. and M.P.-H.; visualization, S.R. and R.F.; supervision, M.P.-H.; funding acquisition, U.O. and M.P.-H. All authors have read and agreed to the published version of the manuscript.

**Funding:** This research was supported by *Spitzencluster it's OWL* and funded by state funds of the Ministry of Economic Affairs, Innovation, Digitalization and Energy of the State of North Rhine-Westphalia (MWIDE.NRW) grant number 005-2011-0117\_AcouMix. The APC was funded by OWL University of Applied Sciences and Arts, Campusallee 12, 32657 Lemgo, Germany.

**Institutional Review Board Statement:** Not applicable.

**Informed Consent Statement:** Not applicable.

**Data Availability Statement:** Not applicable.

**Acknowledgments:** The authors would like to thank the Heinrich-Heine-Universität Düsseldorf, JRS Pharma GmbH & Co. KG, Meggle GmbH & Co. KG, PHARBIL Pharma GmbH—a company of the NextPharma group, and Roquette Frères for providing raw materials. The authors would further like to thank Heinrich Dyck and Kristina Block (PHARBIL Pharma GmbH, Reichenbergerstr. 43, 33605 Bielefeld, Germany) for their support in conducting proof-of-concept experiments. For the support in particle size determination by microscope, the authors would like to thank Volker Salzmann (OWL University of Applied Sciences and Arts, Department of Life Science Technologies, Campusallee 12, 32657 Lemgo, Germany)

**Conflicts of Interest:** The authors declare no conflicts of interest. The funders had no role in the design of the study; in the collection, analyses, or interpretation of data; in the writing of the manuscript; or in the decision to publish the results.

## Abbreviations

The following abbreviations are used in this manuscript:

API	active pharmaceutical ingredient
$\rho_{\text{press}}$	compression density
ratio <sub>lac</sub>	lactose ratio in the dry formulation
$\omega_{\text{wet}}$	water content on wet basis

## Appendix A

**Table A1.** Raw data corresponding to Table 2 and Figure 2. The ratios of the raw materials Lac 200 and MCC 101 refer to the total dry mass, whereas the water content  $\omega_{\text{wet}}$  refers to the total wet mass.

Lac 200 (%)	MCC 101 (%)	$\omega_{\text{wet}}$ (%)
0	100	0
		40
		45
		50
		55
		60
20	80	0
		35
		40
		45
		50
		55

Table A1. Cont.

Lac 200 (%)	MCC 101 (%)	$\omega_{\text{wet}}$ (%)
40	60	0
		30
		33.75
		37.5
		41.25
60	40	45
		0
		25
		28.75
		32.5
80	20	36.25
		40
		0
		15
		18.75
100	0	22.5
		26.25
		30
		0
		2.5
		6.25
		10
		13.75
		17.5

Table A2. Determined residual moisture contents of the dried pellets corresponding to Table 4, Figure 4 and Table 5, Figure 10.

Formulation	$\omega_{\text{wet}}$ (%)	Residual Moisture (%)
80% Lac 200, 20% MCC 101	25.0	0.39
70% Lac 200, 30% MCC 101	28.7	0.79
60% Lac 200, 40% MCC 101	32.4	0.40
60% Lac 200, 40% MCC 101	35.9	0.10
60% Lac 400, 40% MCC 101	31.9	0.31
60% Lac DCL 21, 40% MCC 101	28.8	0.16
60% Man 50 C, 40% MCC 101	31.5	0.22
40% Paracetamol, 40% Lac 200, 20% MCC 101	28.7	0.10

## References

- Hansuld, E.M.; Briens, L. A review of monitoring methods for pharmaceutical wet granulation. *Int. J. Pharm.* **2014**, *472*, 192–201. <https://doi.org/10.1016/j.ijpharm.2014.06.027>.
- Parikh, D.M. (Ed.) *Handbook of Pharmaceutical Granulation Technology*, 2nd ed.; Drugs and the Pharmaceutical Sciences; Taylor & Francis: Boca Raton, FL, USA; London, UK, 2005.
- Kleinebudde, P. The Crystallite-Gel-Model for Microcrystalline Cellulose in Wet-Granulation, Extrusion, and Spheronization. *Pharm. Res.* **1997**, *14*, 804–809. <https://doi.org/10.1023/A:1012166809583>.
- Mort, P.R. Scale-up of binder agglomeration processes. *Powder Technol.* **2005**, *150*, 86–103. <https://doi.org/10.1016/j.powtec.2004.11.025>.
- Leuenberger, H.; Puchkov, M.; Krausbauer, E.; Betz, G. Manufacturing pharmaceutical granules: Is the granulation end-point a myth? *Powder Technol.* **2009**, *189*, 141–148. <https://doi.org/10.1016/j.powtec.2008.04.005>.
- Agrawal, S.; Fernandes, J.; Shaikh, F.; Patel, V. Quality aspects in the development of pelletized dosage forms. *Heliyon* **2022**, *8*, e08956. <https://doi.org/10.1016/j.heliyon.2022.e08956>.
- Leuenberger, H.; Bier, H.P.; Sucker, H. Theory of the granulating-liquid requirement on the conventional granulation process. *Pharm. Technol.* **1979**, *3*, 61–68.

8. Shikata, F.; Kimura, S.; Hattori, Y.; Otsuka, M. Real-time monitoring of granule properties during high shear wet granulation by near-infrared spectroscopy with a chemometrics approach. *RSC Adv.* **2017**, *7*, 38307–38317. <https://doi.org/10.1039/c7ra05252a>.
9. Briens, L.; Daniher, D.; Tallevi, A. Monitoring high-shear granulation using sound and vibration measurements. *Int. J. Pharm.* **2007**, *331*, 54–60. <https://doi.org/10.1016/j.ijpharm.2006.09.012>.
10. Ly, A.; Esmā Achouri, I.; Gosselin, R.; Abatzoglou, N. Wet granulation end point prediction using dimensionless numbers in a mixer torque rheometer: Relationship between capillary and Weber numbers and the optimal wet mass consistency. *Int. J. Pharm.* **2021**, *605*, 120823. <https://doi.org/10.1016/j.ijpharm.2021.120823>.
11. Sakr, W.F.; Ibrahim, M.A.; Alanazi, F.K.; Sakr, A.A. Upgrading wet granulation monitoring from hand squeeze test to mixing torque rheometry. *Saudi Pharm. J.* **2012**, *20*, 9–19. <https://doi.org/10.1016/j.jsps.2011.04.007>.
12. Schwartz, J.B. Granulation. *Drug Dev. Ind. Pharm.* **1988**, *14*, 2071–2090. <https://doi.org/10.3109/03639048809152003>.
13. Alleva, D.S.; Schwartz, J.B. Granulation Rheology I: Equipment Design and Preliminary Testing. *Drug Dev. Ind. Pharm.* **1986**, *12*, 471–487. <https://doi.org/10.3109/03639048609048023>.
14. Chitu, T.M.; Oulahna, D.; Hemati, M. Rheology, granule growth and granule strength: Application to the wet granulation of lactose–MCC mixtures. *Powder Technol.* **2011**, *208*, 441–453. <https://doi.org/10.1016/j.powtec.2010.08.041>.
15. Soh, J.L.P.; Liew, C.V.; Heng, P.W.S. Torque rheological parameters to predict pellet quality in extrusion-spheronization. *Int. J. Pharm.* **2006**, *315*, 99–109. <https://doi.org/10.1016/j.ijpharm.2006.02.023>.
16. Whitaker, M.; Baker, G.R.; Westrup, J.; Goulding, P.A.; Rudd, D.R.; Belchamber, R.M.; Collins, M.P. Application of acoustic emission to the monitoring and end point determination of a high shear granulation process. *Int. J. Pharm.* **2000**, *205*, 79–91. [https://doi.org/10.1016/S0378-5173\(00\)00479-8](https://doi.org/10.1016/S0378-5173(00)00479-8).
17. Gamble, J.F.; Dennis, A.B.; Tobby, M. Monitoring and end-point prediction of a small scale wet granulation process using acoustic emission. *Pharm. Dev. Technol.* **2009**, *14*, 299–304. <https://doi.org/10.1080/10837450802603618>.
18. Papp, M.K.; Pujara, C.P.; Pinal, R. Monitoring of High-shear Granulation using Acoustic Emission: Predicting Granule Properties. *J. Pharm. Innov.* **2008**, *3*, 113–122. <https://doi.org/10.1007/s12247-008-9030-6>.
19. Vorwerk. What is the Rotation Speed of the Thermomix® Blade for the Different Settings? 2018. Available online: <https://support.vorwerk.com/hc/en-gb/articles/360000885809-What-is-the-rotation-speed-of-the-Thermomix-blade-for-the-different-settings-> (accessed on 20 October 2022).
20. Winopal. Schüttgutfestigkeit in Trichtern: Vertikaler Pulver-Schertest. 2018. Available online: <https://www.winopal.com/blog/blogeintraege/schuettgutfestigkeit-in-trichtern-vertikaler-pulver-schertest> (accessed on 12 April 2022).
21. Meggle. Product Configurator. Available online: <https://www.meggle-pharma.de/de/productConfigurator.html> (accessed on 12 April 2022).
22. Nofrerias, I.; Nardi, A.; Suñé-Pou, M.; Suñé-Negre, J.M.; García-Montoya, E.; Pérez-Lozano, P.; Tico, J.R.; Miñarro, M. Comparison between Microcrystalline Celluloses of different grades made by four manufacturers using the SeDeM diagram expert system as a pharmaceutical characterization tool. *Powder Technol.* **2019**, *342*, 780–788. <https://doi.org/10.1016/j.powtec.2018.10.048>.
23. Zhang, J.; Wu, C.Y.; Pan, X.; Wu, C. On Identification of Critical Material Attributes for Compression Behaviour of Pharmaceutical Diluent Powders. *Materials* **2017**, *10*, 845. <https://doi.org/10.3390/ma10070845>.
24. Weyer, K. Beeinflussung und Optimierung von Hilfsstoffeigenschaften durch Interaktion mit Wasser. Ph.D. Thesis, Rheinische Friedrich-Wilhelms-Universität Bonn, Bonn, Germany, 2007.
25. Suzuki, T.; Kikuchi, H.; Yamamura, S.; Terada, K.; Yamamoto, K. The change in characteristics of microcrystalline cellulose during wet granulation using a high-shear mixer. *J. Pharm. Pharmacol.* **2001**, *53*, 609–616. <https://doi.org/10.1211/0022357011775938>.
26. Roberts, R.J.; Rowe, R.C. The compaction of pharmaceutical and other model materials—A pragmatic approach. *Chem. Eng. Sci.* **1987**, *42*, 903–911. [https://doi.org/10.1016/0009-2509\(87\)80048-9](https://doi.org/10.1016/0009-2509(87)80048-9).
27. JRS Pharma. VIVAPUR® Microcrystalline Cellulose. 105. Available online: <https://www.jrspharma.com/pharma-wAssets/docs/brochures/jrs-pharma-mcc-leaflet-vivapur.pdf> (accessed on 25 October 2022).
28. Roquette Frères. MICROCEL® MC-101: Microcrystalline Cellulose. Available online: <https://www.roquette.com/innovation-hub/pharma/product-profile-pages/microcel-mc101-microcrystalline-cellulose> (accessed on 12 April 2022).
29. Wu, J.S.; Ho, H.O.; Sheu, M.T. A statistical design to evaluate the influence of manufacturing factors on the material properties and functionalities of microcrystalline cellulose. *Eur. J. Pharm. Sci.* **2001**, *12*, 417–425. [https://doi.org/10.1016/S0928-0987\(00\)00196-2](https://doi.org/10.1016/S0928-0987(00)00196-2).
30. Carless, J.E.; Leigh, S. Compression characteristics of powders: Radial die wall pressure transmission and density changes. *J. Pharm. Pharmacol.* **1974**, *26*, 289–297. <https://doi.org/10.1111/j.2042-7158.1974.tb09278.x>.